Ultraviolet Raman spectroscopy characterizes chemical vapor deposition diamond film growth and oxidation

Richard W. Bormett and Sanford A. Asher[a)]
University of Pittsburgh, Department of Chemistry, Pittsburgh, Pennsylvania 15260

Robert E. Witowski and William D. Partlow
Westinghouse Science and Technology Center, Pittsburgh, Pennsylvania

Robert Lizewski and Fred Pettit
University of Pittsburgh, Materials Science and Engineering Department, Pittsburgh, Pennsylvania 15260

(Received 3 October 1994; accepted for publication 6 February 1995)

The Raman spectra of diamond and chemical-vapor-deposition (CVD) diamond films in the UV have been excited within the diamond band gap at 228.9 nm for the first time. The lack of fluorescence in the UV-excited Raman spectrum of diamond and CVD diamond films allows Raman spectroscopy to monitor the carbon-hydrogen (C-H) stretching vibrations of the nondiamond components of the CVD film as well as the third-order phonon bands of diamond. The relative intensity of the C-H stretching bands at ~2930 cm^{-1} to the diamond first-order phonon band at 1332 cm^{-1} is proportional to the atomic fraction of covalently bound hydrogen in the CVD diamond film. The third-order phonon band intensity and frequency maxima are very sensitive to the size of the diamond crystallite. Its intensity decreases, and the maximum shifts to lower frequency as the size of the diamond crystallite decreases. It is shown here that UV Raman diamond measurements have significantly greater information content than visible Raman measurements. © *1995 American Institute of Physics.*

I. INTRODUCTION

The recent development of chemical-vapor-deposition (CVD) diamond film growth technology has created the need for fast qualitative and quantitative methods of determining diamond film composition and quality. Raman spectroscopy is an ideal choice for characterizing diamond and other forms of graphitic and amorphous carbon due its sensitivity to different carbon microstructures, which produce distinctive Raman bands for the various forms of carbon.[1,2] For example, the exact frequencies of the Raman bands of diamond, graphite, and amorphous forms of carbon depend upon the size and stresses present in the different carbon domains.[3,4] Numerous Raman studies with excitation in the visible and near-UV region have characterized the Raman spectra of various forms of carbon, and in particular CVD diamond and carbon films. Unfortunately, the strong fluorescence and photoluminescence that accompanies visible and near-UV Raman excitation of CVD diamond generally limits the sensitivity that these Raman excitation wavelengths are able to achieve.

We report here the use of UV Raman excitation in and near the diamond band gap (230 nm) and compare the spectral information content of UV and visible Raman excitation of CVD diamond and diamondlike films. We utilize a newly available intracavity frequency doubled Ar-ion laser and demonstrate the ability to measure fluorescence free spectra with an enhanced detectivity for CVD diamond. The lack of fluorescence in the UV Raman spectra permits us for the first time to monitor both the first- as well as the second- and third-order phonon bands of diamond. The second- and third-order phonon bands of diamond provide additional diagnostic information on the diamond microstructure. UV Raman spectroscopy also detects the C-H stretching bands of nondiamond carbon in CVD diamond films. Information regarding the quantity and type of covalently bound hydrogen in CVD diamond has previously only been available from infrared (IR) spectroscopy. UV Raman measurements below 250 nm were previously not practical due to the photodamage problems associated with the low duty cycle pulsed laser systems that were capable of generating these UV wavelengths. Using a cw intracavity frequency doubled Ar-ion laser with excitation wavelengths at 251, 244, 238, and 228.9 nm we characterized CVD diamond films grown from microwave plasmas containing various oxygen flow rates. Additionally, we monitored the effects of oxidizing environments on the degradation of CVD diamond films. Our UV Raman measurements clearly distinguish three different carbon phases in CVD diamond films which are diamond, glassy carbon, and a hydrogenated amorphous carbon phase.

II. EXPERIMENT

CVD diamond films used in the growth and oxidation study were grown at Westinghouse Science and Technology Center in Pittsburgh, PA. For the oxygen growth study, the diamond films were grown with an ASTeX large area diamond system (LADS) on a silicon substrate with a furnace temperature of 850 °C to a thickness of ~10–20 μm. The gas feed for the plasma consisted of a mixture of hydrogen, methane, carbon dioxide, and oxygen. The hydrogen, methane, and carbon dioxide flow rates were 700, 100, and 100 sccm, respectively. The oxygen flow rate was varied from 15 to 60 sccm. The CVD diamond films were left on the silicon substrate for the Raman measurements.

[a)]Electronic mail: ASHER@VMS.CIS.PITT.EDU

 0021-8979/95/77(11)/5916/8/$6.00

The CVD diamond used in the oxidation study was grown at Westinghouse STC with an in-house-built dc arc plasma reactor. The CVD diamond was grown on a Mo substrate that was removed by a HF acid etch. The CVD film was fractured to sizes of approximately 3×3 mm^2 and sorted according to quality as determined by scanning electron spectroscopy (SEM) and UV Raman spectroscopy. The CVD diamond was oxidized at 1 atm at 600 °C in a flowing ultrahigh-purity oxygen atmosphere for 2, 4, or 8 min. The CVD diamond was characterized after oxidation with both SEM and UV Raman spectroscopy.

The UV (228.9 and 244 nm) and visible (488 nm) Raman spectra were excited with a Coherent, Inc., model 301 Ar^+ laser equipped with an intracavity frequency doubler.[5] The Raman scattered light was collected in a backscattering geometry and imaged into a SPEX 1877B Triplemate or SPEX 1401 double spectrograph equipped with an EG&G PAR 1420 blue intensified photodiode array and optical multichannel analyzer. The 488 and 244 nm excited Raman spectra were obtained with resolutions of ~4 cm^{-1}. The 228.9 nm Raman spectra were measured with a decreased ~25 cm^{-1} resolution in order to simultaneously measure the first-, second-, and third-order Raman bands.

The highly ordered pyrolytic graphite (HOPG) and glassy carbon (GC20) were gifts from Professor McCreery of Ohio State University.[2] Different crystalline and microcrystalline graphite powders and diamond powders (40–60 μm and <1 μm) were purchased from Alfa. The large single-crystal natural diamond used for Raman spectral comparison was a type-IIa polished gem from an engagement ring. The UV-visible absorption spectrum was measured for a type-IIa 2-mm-thick polished diamond substrate borrowed from Professor Yates of the University of Pittsburgh.

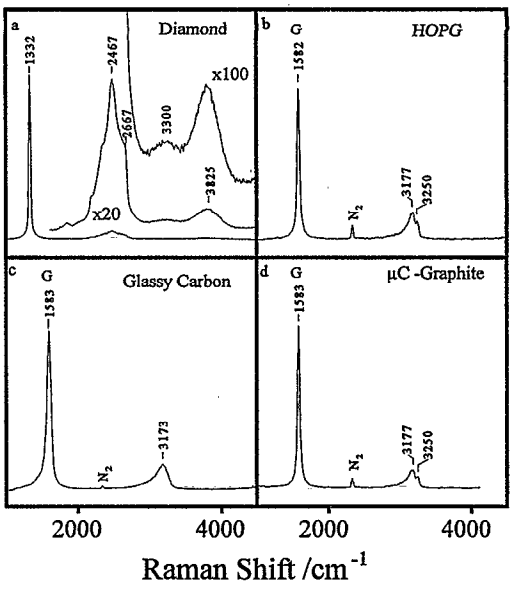

FIG. 1. 228.9 nm excited Raman spectra of (a) gem quality diamond, (b) HOPG, (c) GC20 glassy carbon, (d) microcrystalline graphite (<1 μm). The spectra were obtained with 2–5 mW of laser power focused to ~25 μm spot size with total integration times of 1–3 min and a spectral resolution of ~25 cm^{-1}.

III. RESULTS AND DISCUSSION

A. Comparison of visible and UV excitation

The 228.9 and 488 nm excited Raman spectra of various carbon forms [natural diamond, HOPG, microcrystalline graphite, and glassy carbon (GC20)] are shown in Figs. 1 and 2, respectively. Figures 1(a) and 2(a) show the UV and visible excited Raman spectra of a polished type-IIa gem quality diamond. The Raman spectrum can be separated into three regions based on the number of phonons involved in the scattering process. The first-order phonon spectrum results from the scattering of a single optical phonon at the maximum in the density-of-states function of diamond which occurs at the center of the Brillouin zone.[6] The 1332 cm^{-1} triply degenerate band is the only allowed Raman band in the first-order diamond spectrum; for a type-IIa single crystal it has a full width at half-height (FWHH)[6] of ~1.7 cm^{-1}. For microcrystalline diamond relaxation of the conservation of momentum selection rule allows scattering from lower-frequency phonons near the maximum of the density-of-states function. The scattering from lower-frequency phonons near the center of the Brillouin zone of microcrystalline diamond downshifts the 1332 cm^{-1} band frequency and increases the FWHH.[3]

Two phonon scattering processes in diamond produce a higher-frequency broad complex band with a maximum at 2467 cm^{-1} and a sharp cutoff at 2667 cm^{-1}. The second-order phonon band of diamond consists primarily of overtone and combination bands of phonons at high symmetry points in the Brillouin zone.[6] Peaks and discontinuities in the

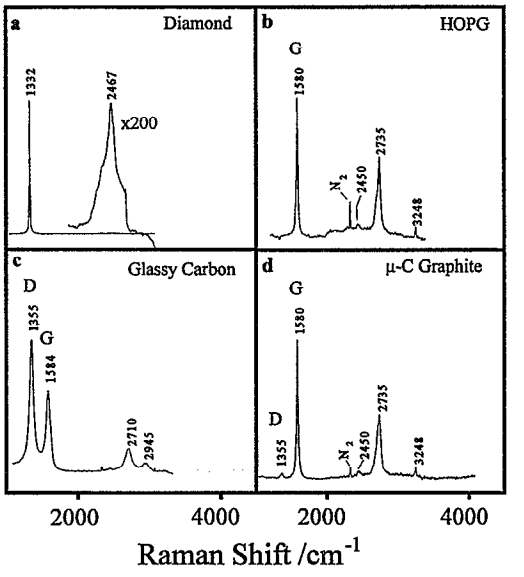

FIG. 2. 488 nm excited Raman spectra of (a) gem quality diamond, (b) HOPG, (c) GC 20 (glassy carbon), (d) microcrystalline graphite (<1 μm). The diamond spectrum was obtained with 80 mW and the graphite spectra with 800 mW of laser power focused to ~25 μm spot size. The integration times for diamond were 10 and 100 s for the first- and second-order spectra, respectively, and 2 min for the graphite materials. The spectral resolution is ~15 cm^{-1}.

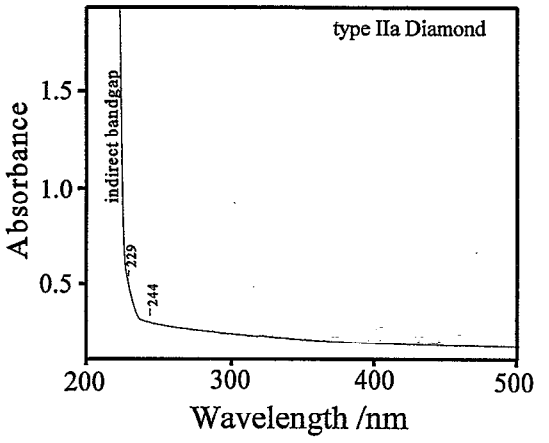

FIG. 3. UV-VIS absorption spectrum of a 2-mm-thick type-IIa diamond substrate.

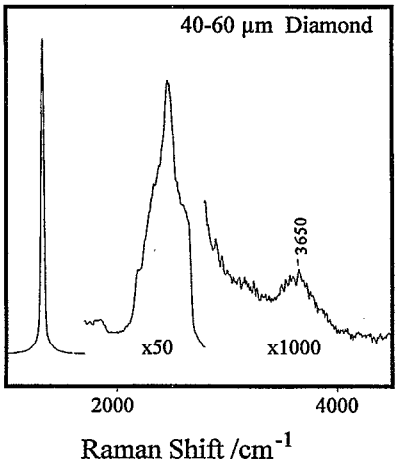

FIG. 4. 228.9 nm excited Raman spectrum of 40–60 μm natural diamond powder. Acquisition conditions were identical to those in Fig. 1

second-order spectrum also occur at frequencies that correspond to the critical points in the density-of-states function of diamond. Careful measurement of the second-order phonon spectrum allows accurate determination of phonon energies and symmetries of high-symmetry points and critical points in the Brillouin zone.[6] Figures 1(a) and 2(a) show that for UV excitation the second-order phonon spectrum of diamond has a peak intensity approximately 20 times weaker than the first-order phonon band; however, the second-order phonon band is ~200 times weaker for visible excitation.

The higher UV Raman relative intensity of the diamond second-order phonon band with respect to the diamond first-order phonon band results from significant resonance enhancement of the second-order phonon band compared to the first-order band as the excitation wavelength approaches the band gap of diamond.[7] Figure 3 shows the absorption edge for a type-IIa diamond compared to the UV Raman excitation wavelengths used in this study. While previous UV Raman diamond studies have approached this indirect band gap,[7,8] our 228.9 nm excitation is to our knowledge the first Raman measurement actually within the band gap.

Figure 1(a) shows the first spectrum of the third-order phonon scattering in diamond which gives rise to a broad Raman band at ~3800 cm^{-1}. The diamond third-order phonon Raman spectrum has not previously been reported because of its vanishingly weak intensity with visible Raman excitation and because of fluorescence interference. The third-order phonon spectrum of a large type-IIa single-crystal diamond shows a maximum at 3825 cm^{-1} and the expected third-order density of states cutoff at ~4000 cm^{-1}. Figure 1(a) shows that the third-order spectrum has at least one additional low-energy shoulder at ~3300 cm^{-1}. The frequency, band shape, and intensity of the third-order diamond phonon band is very sensitive to the diamond crystal size. Figure 4 shows the 228.9 nm Raman spectrum of a 40–60 μm natural diamond powder. For microcrystalline diamond the intensity maximum of the third-order phonon band shifts from 3825 to 3650 cm^{-1} and the intensity decreases an order of magnitude with respect to the diamond first-order phonon band.

CVD diamond often contains appreciable amounts of nondiamond carbon that exhibits Raman bands characteristic of graphite or highly disordered sp^2 and sp^3 carbon. The first-order 1582 cm^{-1} phonon band (G band) of HOPG with 228.9 and 488 nm excitation is shown in Figs. 1(b) and 2(b), respectively. The G band results from an in-plane graphite vibration of E_{2g} symmetry.[2,9] The graphitic Raman spectrum is strongly affected by graphitic ordering. The 488 nm excited first-order phonon spectra of microcrystalline graphite [Fig. 2(d)] and glassy carbon [Fig. 2(c)] show that the width of the G band increases and that a band at 1355 cm^{-1} (D band) appears when the graphite becomes microcrystalline or highly disordered as in glassy carbon. It is well established that the D band results from the presence of graphitic edge planes.[2] The G to D band relative intensity has previously been used to determine the average size of the graphitic crystallites, since smaller graphitic crystallites expose more edge plane.[4,9] The absence of the D band in the 228.9 nm excited Raman spectra of graphite materials follows the trend shown by other researchers in which the D band intensity decreases as the excitation frequency increases.[2,8,10] Since the D band from graphitic carbon does not appear in the UV Raman spectra, the diamond Raman first-order phonon spectrum is easily obtained without interference even for poor quality CVD diamond films with a relatively large nondiamond concentration.

The UV-excited second-order phonon spectra of HOPG and microcrystalline graphite show the 3175 cm^{-1} G band overtone and the 3250 cm^{-1} overtone of a Raman forbidden band (~1620 cm^{-1}). The UV second-order phonon spectrum of glassy carbon shows only a broad single band without resolution of separate maxima for the 3175 and 3250 cm^{-1} overtones. The 488 nm excited second-order phonon spectra of HOPG and microcrystalline graphite show three overtone bands at 3250, 2735, and 2450 cm^{-1} for the first-order Raman forbidden phonons at 1620, 1360, and 1225 cm^{-1}.[2] The 488 nm excited second-order phonon spectrum of glassy carbon shows an additional Raman band at ~2945 cm^{-1}. The absence of the graphite second-order phonon bands (2450,

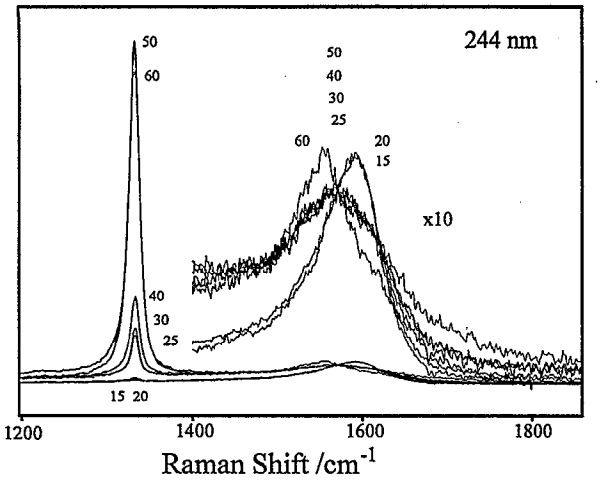

FIG. 5. 244 nm excited Raman spectra of microwave-grown CVD diamond films grown with 15, 20, 25, 30, 40, 50, and 60 sccm oxygen flow rates measured with ~50 mW focused to a ~25 μm spot size with a total integration times of 100 s; the spectral resolution is 4 cm^{-1}. The data have been normalized to give identical Raman intensities at 1570 cm^{-1}.

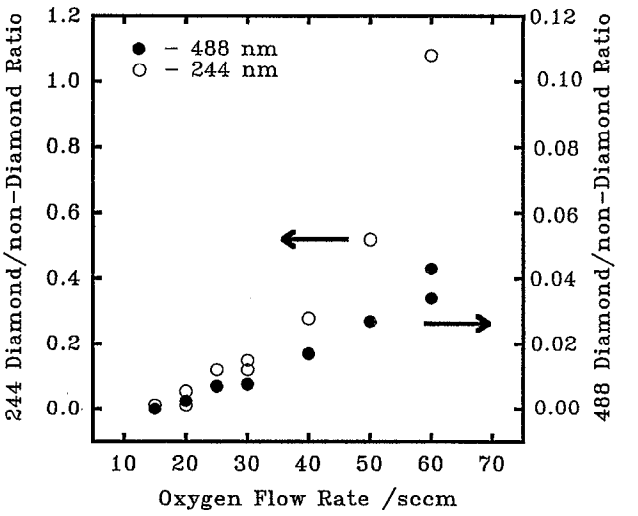

FIG. 7. Ratio of the integrated intensities of the diamond to nondiamond Raman bands shown in Fig. 5 (244 nm:○) and Fig. 6 (488 nm: ●).

2710, and 2945 cm^{-1}) with UV excitation allows the diamond second-order phonon band (2467 cm^{-1}) and the carbon-hydrogen (C-H) stretching bands of nondiamond carbon (~2930 cm^{-1}) to be monitored in CVD diamond films.

B. CVD film studies

The ability of UV Raman to monitor both the relative amounts of diamond and the C-H bound hydrogen in CVD films, is demonstrated in the spectra of CVD films grown with an increasing oxygen content in a microwave plasma; figs. 5 and 6 show the 244 and 488 nm excited Raman spectra, respectively, of CVD films grown with oxygen flow rates ranging from 15 to 60 sccm. The relative intensity of the spectra have been normalized to the intensity of the nondiamond carbon Raman band at 1570 cm^{-1}. The 244 nm Raman spectra (Fig. 5) show a distinct diamond phase for all gas mixtures used in this study, in contrast to the 488 nm Raman spectra (Fig. 6) that do not show a clear diamond phase until the oxygen flow rates exceeds 20 sccm. Figures 5 and 6 show that the intensity of the 1332 cm^{-1} diamond band relative to that of the ~1580 cm^{-1} nondiamond band dramatically increases with UV excitation compared to visible excitation. The increase in the relative intensity of the diamond band to the nondiamond band in the UV Raman spectrum does not result from resonant enhancement of the first-order diamond phonon band but rather from the decreased relative Raman cross section for the nondiamond carbon band. The ratios of the integrated intensity of the diamond band to nondiamond carbon band calculated from Figs. 5 and 6 are shown in Fig. 7. The 244 nm Raman intensity ratio of the diamond to nondiamond carbon bands is ~25-fold larger than is the 488 nm Raman intensity ratio. Additionally, Fig. 6 shows that the visible Raman spectra of the CVD films used in this study are complicated by the presence of a strong fluorescence signal that increases as the oxygen flow rate increases. The strong fluorescence signal required a base-line correction that was not always linear for determining peak areas and limited the maximum signal-to-noise (S/N) ratio of the Raman measurement.

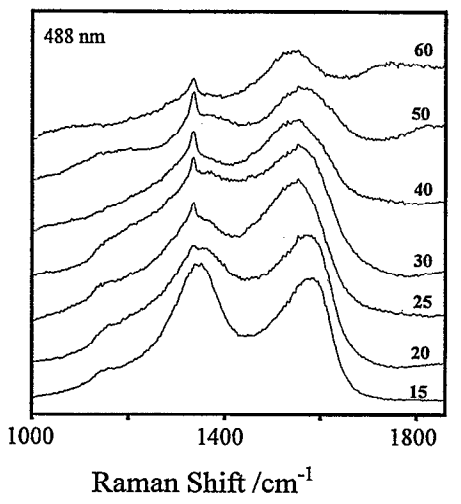

FIG. 6. 488 nm excited Raman spectra of microwave-grown CVD diamond films grown at 15, 20, 25, 30, 40, 50, and 60 sccm oxygen flow rates measured with ~800 mW laser power focused to 25 μm. The spectra were acquired with a total 100 s integration time at 4 cm^{-1} resolution. The spectra have been normalized to the Raman intensity at 1570 cm^{-1}.

The dependence of the Raman spectra of the nondiamond and diamond components of CVD diamond films as a function of excitation wavelength was previously examined with excitation in the near-UV spectral region.[2,8,10] These studies showed that as the Raman excitation frequency increase the relative Raman cross sections of the nondiamond or graphitic components decreases; in addition, the frequencies of the first-order bands of nondiamond carbon (~1550 cm^{-1}) increase while the *D* band at 1355 cm^{-1} and its overtone and combination bands at 2450, 2725, and 2950 cm^{-1} disappear. Our UV Raman measurements below 250 nm show that these spectral trends continue to 228.9 nm. Al-

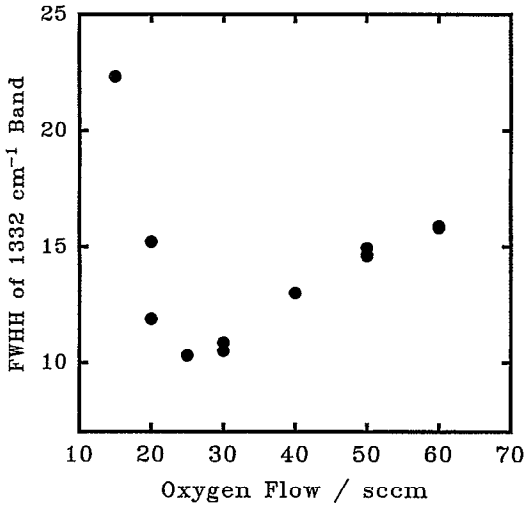

FIG. 8. Measured bandwidth of the 244 nm excited first-order diamond phonon band of the microwave-grown CVD films shown in Fig. 5. The duplicate Raman spectra were measured for two different areas of the 20, 30, and 50 sccm oxygen grown films.

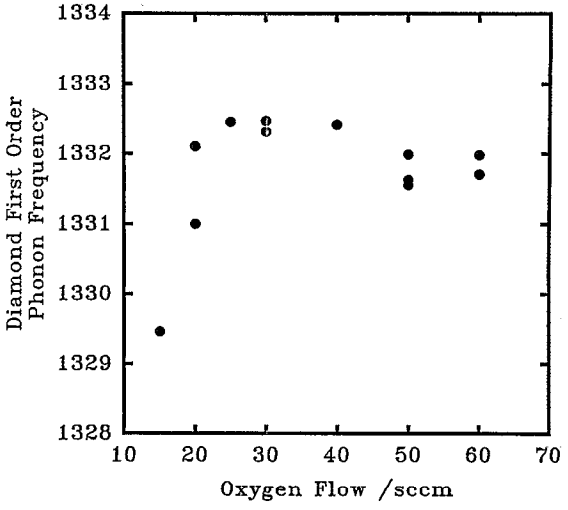

FIG. 9. Measured Raman shift of the 244 nm excited first-order diamond phonon band of the microwave-grown CVD films shown in Fig. 5.

though the relative Raman cross section of the nondiamond component of the CVD diamond film decreases with UV excitation, the spectral S/N ratio increases compared to visible excitation due to the elimination of interfering fluorescence. Even for high-purity CVD diamond where the concentration of nondiamond impurities is very small, the high S/N ratio UV Raman spectra allow quantitative determination of the nondiamond carbon and C-H bound hydrogen.

The higher S/N ratio of the UV Raman spectra of the microwave grown films allows a very accurate measure of bandwidth and frequency of the diamond first-order phonon band. Figure 8 shows the diamond first-order phonon bandwidth as a function of the oxygen flow rate. The first-order diamond phonon bandwidth decreases from 22 cm^{-1} for the 15 sccm oxygen grown film to 10 cm^{-1} for the 25 sccm oxygen grown film. The increase in oxygen flow beyond 25 sccm increases the diamond first-order diamond phonon bandwidth to 16 cm^{-1} for the highest oxygen (60 sccm) flow rate. The increase in the diamond first-order phonon bandwidth from 25 to 60 sccm oxygen occurs despite the appearance in the SEM measurements of highly faceted crystallites and an apparently purer diamond film at the higher oxygen flow rates. The diamond first-order phonon bandwidth is a sensitive measure of the diamond scattering domain size as determined by stacking faults and crystal twinning in the diamond crystallites.[3] The LeGrice *et al.* relationship that correlates domain size to bandwidth, allows us to calculate a domain size of less than 40 Å for the 15 sccm oxygen grown CVD film and 70 Å size for the 25 sccm oxygen flow rate. Despite the higher purity of the 60 sccm grown CVD diamond, the domain size appears to be smaller than for the poorer quality CVD films. This probably results from a higher crystal defect density caused a high oxidative etching rate and subsequent renucleation of diamond during the growth process.

Figure 9 shows the frequency of the diamond first-order phonon band for the CVD films as a function of the oxygen flow rate. The diamond first-order phonon frequency varies from the minimum of 1329.5 cm^{-1} for the 15 sccm oxygen grown film to a maximum at 1332.8 cm^{-1} for 30 sccm grown film. The frequency of the diamond first-order phonon band decreases for higher oxygen flow rates to ~1332.5 cm^{-1}. The diamond first-order phonon frequency is a function of stress for large single crystals and a function of domain size and stress for crystallite domains smaller than ~1 μm.[3,11] Residual stress in CVD diamond films is difficult to avoid due the elevated temperatures at which the film is grown and the differences in the coefficient of thermal expansion (CTE) for diamond and the growth substrate. Since the CVD film is comprised of more than one type of carbon, calculations of the expected stress are difficult. For example, the CTE for silicon is 2.6×10^{-6}/°C; graphite has a CTE that depends on the crystallographic direction (8.8×10^{-6}/°C in plane and 27.3×10^{-6}/°C along the c axis), while diamond has a temperature-dependent CTE ranging from 0.4×10^{-6}/°C at 193 K to 1.5×10^{-6}/°C at 400 K.[12]

Since the first-order phonon band frequency is affected by both the film stress and the crystallite domain size, any film stress calculation must correct for the frequency down shift resulting from the small crystallite domain size.[3] The stress is then directly proportional to the change in the peak position, $\Delta\nu=\nu_0-\nu_s$, where ν_0 and ν_s are the natural unstressed and stressed phonon frequencies, respectively.[11] Although the size of the first phonon peak shift depends on the crystallographic direction of the stress, the average peak shift for stress along ⟨111⟩ (−2.63 cm^{-1}/GPa) and ⟨100⟩ (−1.08 cm^{-1}/GPa) provides an estimate of the stress and the relative change in stress for the CVD films since the SEM micrographs of the CVD films show a highly random crystallite orientation. Figure 10 shows the stress calculated for the domain size corrected frequency as a function of oxygen flow rate. Although there is a large amount of scatter in this stress data, the trend suggests an increased compressive stress as the oxygen flow rate increased.

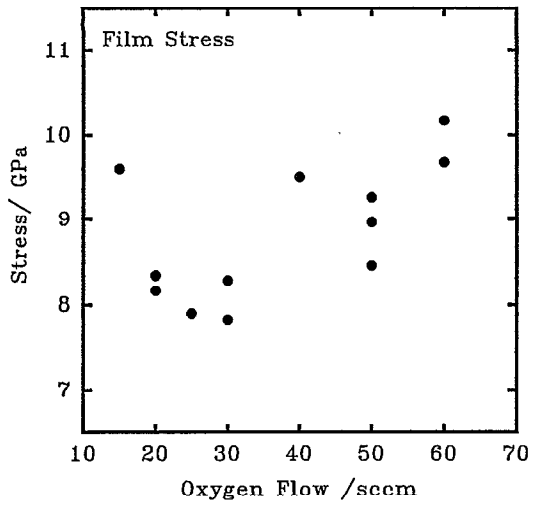

FIG. 10. Stress of the microwave-grown CVD diamond films calculated from the domain size-corrected position determined with the 244 nm Raman excitation and the average value for ⟨111⟩ and ⟨100⟩ uniaxial stress shifts obtained from Ref. 11.

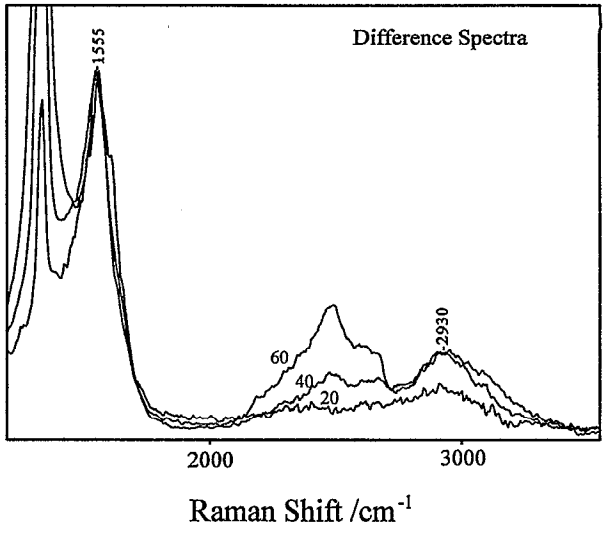

FIG. 12. 228.9 nm Raman difference spectra of microwave-grown CVD diamond films grown at 20, 40, and 60 sccm oxygen flow rates minus that of the 15 sccm oxygen grown film.

The most striking advantage of UV Raman excitation is the lack of fluorescence. This lack of fluorescence allows the monitoring of the second-order diamond and nondiamond carbon Raman spectrum in the CVD films. Of particular interest is the diamond second-order phonon region and the C-H stretching or graphite second-order phonon region. Figure 11 shows the 228.9 nm excited Raman second-order spectra of the CVD films grown in the oxygen flow study. The first- and second-order nondiamond bands of the 15 sccm oxygen grown film have similar frequencies to the graphite G band and overtone and the overtone band of glassy carbon but have larger bandwidths. As the oxygen content of the feed gas increases from 15 sccm, the intensities of the graphite like first- and second-order phonon bands at 1585 and 3160 cm^{-1} decrease relative to the diamond bands and an additional band near ~2945 cm^{-1} appears. The 2470, 3160, and 2945 cm^{-1} bands clearly show the presence of at least three distinct carbon species, which include diamond, graphite, and presumably amorphous hydrogenated carbon.

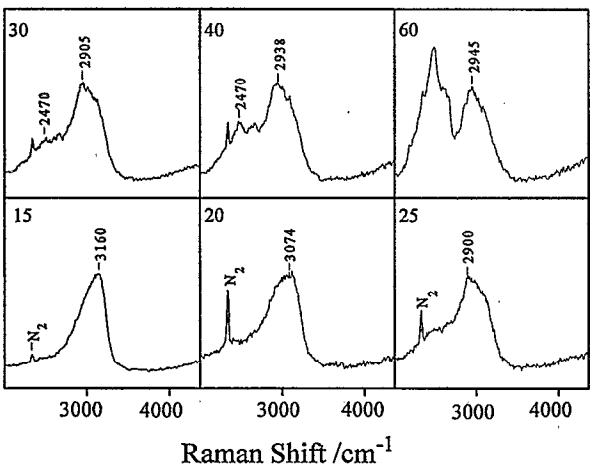

FIG. 11. 228.9 nm excited second-order phonon spectra of microwave-grown CVD diamond films grown with 15, 20, 25, 30, 40, and 60 sccm oxygen flow rates. Laser power and resolution are identical to those for Fig. 1.

C. UV Raman studies of covalently bound hydrogen

Pure graphite materials do not produce a UV Raman band at 2945 cm^{-1}, thus the ~2945 cm^{-1} UV Raman band must result from the overlap of C-H stretching vibration from sp^3, sp^2, or sp^1 carbon. In the absence of a large graphite second-order band the area of the ~2945 cm^{-1} C-H stretching vibration is easily calculated and provides a means of quantitating the amount of C-H hydrogen in CVD diamond films. The hydrogen content of CVD diamond films is typically determined with IR-absorption measurements of C-H stretching bands, but thin-film interference effects and the weak C-H absorption of high-purity films often make IR quantitation difficult. The nondiamond carbon UV Raman spectra of the 20, 40, and 60 sccm grown films after subtraction of the 15 sccm nondiamond carbon spectrum (Fig. 12) shows a nondiamond carbon band at 1555 cm^{-1} and a ~2930 cm^{-1} C-H stretching band.

Since the CVD films are predominantly diamond, the ratio of the diamond first-order phonon band intensity to the 2930 cm^{-1} C-H stretching band intensity is proportional to the atomic percentage of hydrogen in the CVD diamond films. Figure 13 compares the atomic percentage of hydrogen determined by IR spectroscopy[13] with the ratio of the 2930 cm^{-1} C-H band area I_{2930} to the 1332 cm^{-1} diamond band area I_{1332} as a function of oxygen flow rate. For 228.9 nm excitation the atomic percentage of hydrogen can now be obtained from: $\%H=K(I_{2945}/I_{1332})$, where K is calculated from Fig. 13 to be 2.5 hydrogen atom percent. We have measured I_{2945}/I_{1332} ratios of less than 4×10^{-4} for CVD

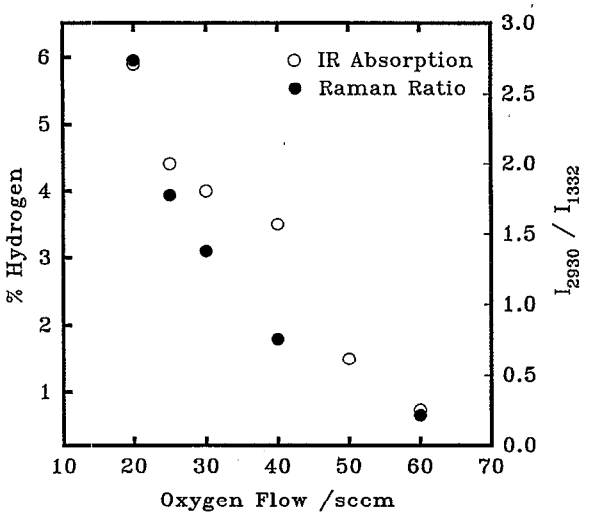

FIG. 13. Comparison of the oxygen flow rate dependent atomic percentage of hydrogen for the microwave-grown CVD diamond films calculated with an IR-absorption coefficient of 1.7×10^{21} cm^{-2} (Ref. 13: ○) with the ratio of the Raman C-H stretching band area to the first-order diamond phonon band area for 228.9 nm excitation (●).

films that showed no measurable C-H stretching IR absorption. This represents a detection limit of ~0.001% atomic hydrogen.

D. Nondiamond carbon oxidation

The degradation behavior of CVD diamond films in oxidizing environments often depends on the nature and quantity of nondiamond impurities. We characterized the effects of an oxidizing environment on the diamond and nondiamond components of CVD diamond. The diamond is monitored by the 1332 and 2460 cm^{-1} bands and the nondiamond carbon by the ~1575 and 2930 cm^{-1} bands. Figure 14 shows the 244 nm excited Raman spectra of CVD diamond measured before and after 2, 4, and 8 min of oxidation in a pure oxygen atmosphere at 600 °C. The Raman spectra have been normalized to have the same integrated intensity for the diamond first-order phonon band.

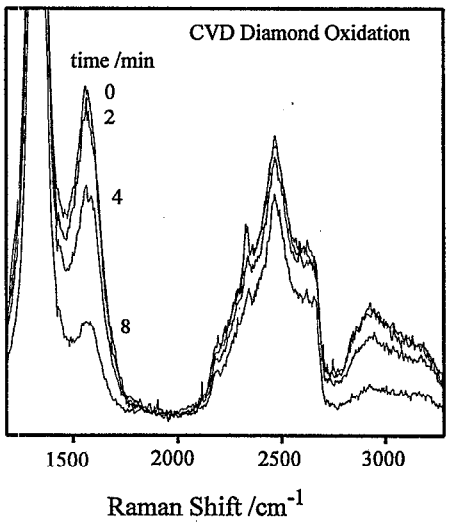

FIG. 14. 228.9 nm excited Raman spectra of dc arc-grown CVD diamond film after oxidation for 0, 2, 4, 8 min in a pure oxygen atmosphere at 600 °C. The spectra were obtained with 10 mW of laser power focused to a ~25 μm spot size with total integration times of 5 min and a spectra resolution of ~ 25 cm^{-1}.

The integrated Raman intensities of the diamond and nondiamond first-order phonon bands after 2 min of oxidation show only a small decrease in the intensity of the ~1575 cm^{-1} nondiamond Raman band. No changes were observed in the integrated intensity ratios of the second-order bands. After 4 min of oxidation the integrated intensities of both the 1575 and 2930 cm^{-1} bands associated with nondiamond carbon decrease in intensity relative to the diamond first- and second-order phonon bands. The relative intensities of the nondiamond carbon bands continue to decrease with respect to the diamond first-order phonon band with 8 min of oxidation. Additionally, at 8 min of oxidation the diamond film shows a decrease in the integrated intensity of the diamond second-order phonon band relative to the diamond first-order phonon band.

The different initial response of the nondiamond Raman bands at 1575 and 2930 cm^{-1} shows that more than one type of nondiamond carbon exists in the CVD film. The two nondiamond carbon phases contribute unequally to the observed Raman intensity at ~1575 and 2930 cm^{-1}. The more rapidly oxidized nondiamond phase most likely corresponds to nondiamond carbon that occurs on the growing crystallite facets as a single monolayer of defective diamond, while the material which occurs along the columnar boundaries that extend into the film, oxidizes more slowly due to its reduced surface area with respect to the oxidizing environment. While the 8 min oxidized diamond film shows the expected decrease in Raman intensity for the nondiamond carbon, it also shows an unexpected intensity decrease of the diamond second-order band at 2460 cm^{-1}. It is not clear why the diamond second-order band decreases in intensity relative to the diamond first-order band, but it could result from a change in the dominant diamond crystallite orientation. Since the first- and second-order phonon bands of diamond are strongly polarized, the preferential oxidation of a particular diamond growth surface could lead to an apparent decrease in the relative intensities of the diamond first- and second-order phonon bands. An alternative explanation involving a decrease in the sampled crystallite size can be ruled out since the diamond first-order phonon bandwidth does not change.

IV. CONCLUSION

Visible Raman spectroscopy has been an essential tool for the characterization and identification of CVD diamond and diamondlike films, but the signal to noise ratio of the visible Raman data is often decreased by strong fluorescence of highly defective diamond. We show here that cw UV lasers now allow the acquisition of Raman spectra where fluorescence and photoluminescence do not interfere, and resonance Raman enhancement increases the information content of the Raman data. We measure the third-order phonon bands of diamond which is particularly sensitive to the diamond crystallite size. We also demonstrate the ability to use UV

Raman to measure the C-H stretching bands of nondiamond carbon and to determine the atomic percentage of hydrogen in CVD diamond films. The ability to measure fluorescence free spectra and measure the C-H stretching bands makes UV Raman spectroscopy the method of choice for monitoring and characterizing both high- and low-quality CVD diamond and diamondlike films. This approach will be ideal for *in situ* measurements of growing diamond films.

ACKNOWLEDGMENTS

We gratefully thank Westinghouse Science and Technology Center for the diamond films, Professor Richard McCreery for the graphite samples, and Professor John Yates for the loan of the type-IIa diamond. We thank Ann Bormett for the loan of the diamond from her engagement ring. This work was supported by the AFOSR grant to the University of Pittsburgh Materials Research Center (F49620-94-1-0268), and Westinghouse Corporation.

[1] D. S. Knight and W. B. White, J. Mater. Res. **4**, 385 (1989).
[2] Y. Wang, D. C. Alsmeyer, and R. R. McCreery, Materials **2**, 557 (1990).
[3] Y. M. LeGrice, R. J. Nemanich, J. T. Glass, Y. H. Lee, R. A. Rudder, and R. J. Markunas, Mater. Res. Soc. Symp. **162**, 219 (1990).
[4] R. J. Nemanich and S. A. Solin, Phys. Rev. B **20**, 392 (1979).
[5] S. A. Asher, R. W. Bormett, X. G. Chen, D. H. Lemmon, N. Cho, P. Peterson, M. Arrigoni, L. Spinelli, and J. Cannon, Appl. Spectrosc. **47**, 628 (1993).
[6] S. A. Solin and A. K. Ramdas, Phys. Rev. **1**, 1687 (1970).
[7] J. M. Calleja, J. Kuhl, and M. Cardona, Phys. Rev. B **17**, 876 (1978).
[8] J. Wagner, M. Ramsteiner, C. Wild, and P. Koidl, Phys. Rev. B **40**, 1817 (1989).
[9] F. Tuinstra and J. L. Koenig, J. Chem. Phys. **53**, 1126 (1970).
[10] J. Wagner, C. Wild, and P. Koidl, Appl. Phys. Lett. **59**, 779 (1991); M. Yoshikawa, G. Katagiri, H. Ishida, and A. Ishitani, J. Appl. Phys. **64**, 6464 (1988); M. Ramsteiner and J. Wagner, Appl. Phys. Lett. **51**, 1355 (1987).
[11] M. H. Grimsditch, E. Anastassakis, and M. Cardona, Phys. Rev. B **18**, 901 (1978); M. Yoshikawa, G. Katagiri, H. Ishida, and A. Ishitani, Appl. Phys. Lett. **55**, 2608 (1989).
[12] M. N. Yoder in *Diamond Films and Coatings Development, Properties and Applications*, edited by Robert F. Davis (Noyes, Park Ridge, NJ, 1993), p. 4.
[13] N. Kenji, S. Ueda, M. Kumeda, A. Morimoto, and T. Shimizu, Jpn. J. Appl. Phys. **21**, L176 (1982).